IOP Conference Series: Materials Science and Engineering

PAPER • OPEN ACCESS

Prediction of the strength of high entropy alloys of the Al-Cr-Nb-Ti-V-Zr system by the solid-solution hardening model

To cite this article: D N Klimenko *et al* 2021 *IOP Conf. Ser.: Mater. Sci. Eng.* **1014** 012017

Prediction of the strength of high entropy alloys of the Al-Cr-Nb-Ti-V-Zr system by the solid-solution hardening model

D N Klimenko*, N D Stepanov, S V Zherebtsov

Laboratory of Bulk Nanostructured Materials, Belgorod State University, Belgorod, 308015, Russia

*Corresponding author: klimenko@bsu.edu.ru

Abstract. An approach based on the phase prediction of both the phase composition and the solid solution hardening was investigated. This approach showed good agreement between the calculated and experimental values of the yield strength at 20 and 600 °C.

1. Introduction

High entropy alloys (HEAs) usually consist of at least 5 elements in approximately equimolar proportions [1]. It was believed that the high entropy of such alloys resulted in the formation of face-centered cubic (FCC) or body-centered (BCC) solid solutions [2]. Although this idea has not been fully worked out, some of HEAs have a single-phase microstructure with a very good combination of properties [3]. For example, HEAs based on refractory elements demonstrate remarkable high temperature strength, outperforming currently used nickel-based superalloys [4-5], suggesting the potential application of these HEAs as material for the production of high temperature parts.

The main strengthening mechanisms of metal and alloys comprise grain boundary strengthening, solid solution strengthening, precipitation hardening and dislocation strengthening. Considering refractory high entropy alloys (RHEA) with a single-phase BCC metallic solid solution (or with only a very small amount of second phases) it can be suggested that solid solution hardening (SSH) contributes mainly to the yield strength in RHEAs. The range of models based on classical approaches for binary systems and multicomponent alloys [8,9] for calculation of SSH in HEAs were proposed in [4-7]. The combination of solid-solution hardening models with empirical rules and CALPHAD modeling can serve as a basis for predicting the phase composition of alloys and development an approach to creating high-strength HEAs. Therefore, the goal of this work was evaluation of this approach for searching Al-Cr-Nb-Ti-V-Zr system high-strength alloys.

2. Materials and experimental details

Model alloys for the testing model were chosen in three stage. Grid search in the Al - Cr - Nb - Ti - V – Zr system was done in the range of concentrations of 0-15% with a step of 1% for Al and Cr and in the range of concentrations of 0-45% with a step of 5% for other elements. At the first stage, a set of alloys was chosen using the criteria of the single-phase alloy formation: atomic size mismatch $\delta<5.4\%$, valence electron concentration VEC< 6.87, enthalpy of mixing ΔH_mix = -16.25 – 4 kJ/mole [10]. Then, the solid-solution hardening was calculated at 20 and 600 °C for the selected alloys. The calculations solid solution hardening calculations were carried out using an approach described in [7]. At the last stage,

thermodynamic modeling of equilibrium phase diagrams was conducted using the Thermo-Calc 2019 software with the HEA3 (high entropy alloys) database.

The model alloys were produced by vacuum arc melting, using proper mixtures of pure metals with purities higher than 99.9 wt.%, in Ti-gettered argon atmosphere. The measured compositions of the model alloys are listed in Table 1. The alloys were remelted five times to improve their homogeneity. The obtained ingots were sealed in vacuumed (10^{-2} torr) quartz tubes, and then homogenized at 1200 °C for 10 h. After homogenization annealing, the ingots were cut off using an electrical discharge machine into samples for compression test and microstructure investigation.

Table 1. Chemical compositions (at.%) of the model alloys.

Alloys	Al	Cr	Nb	Ti	V	Zr
A1	13.6	13.1	23.4	22.4	25	2.5
A2	11.8	1.9	18.8	44.5	15.8	7.2
A3	14.6	11.5	6.2	37	21	9.7
A4	11.2	6.3	8	49.2	13.9	11.4
A5	11.7	0	9.7	44.8	29.1	4.7
A6	11.8	0.9	22.1	30.5	20.4	14.3
A7	13.6	3	20.6	34	4	24.8
A8	9	0	20.3	36.2	13.8	20.7

Rectangular specimens in size 8×5×5 mm^3 were compressed using an Instron 300LX testing machine equipped with a radial heating furnace. The tests were carried out at temperatures 22 or 600 °C with an initial strain rate of 10^{-4} s^{-1} till 50% height reduction (or till fracture).

The microstructure of the homogenized alloys was studied using X-ray diffraction (XRD) and scanning electron microscopy (SEM) equipped with energy-dispersive X-ray spectrometry (EDS). Specimens for structural investigations were finished with OP-S suspension (the abrasive particle size of 0.04 μm). The chemical composition of the alloys was measured using an SEM-EDS with a scanning area of 2×2 mm^2.

Microhardness was measured using a Wolpert group 402mvd microhardness tester. The load and dwell time were 300 g and 10 s, respectively. The microhardness value was averaged on measurements in five distinct regions.

3. Results of prediction and experimental studies

The solid solution hardening of the model alloys was calculated using the equations given in Ref. [7]:

$$\sigma = F_\tau Z M \mu$$

$$M = (x_1 \dots . x_n) \begin{pmatrix} 0 & (\xi\sqrt{\{\eta_1'^2\}^2 + \{\alpha\delta_1^2\}^2})^{4/3} & (\xi\sqrt{\{\eta_1'^n\}^2 + \{\alpha\delta_1^n\}^2})^{4/3} \\ (\xi\sqrt{\{\eta_2'^1\}^2 + \{\alpha\delta_2^1\}^2})^{4/3} & 0 & (\xi\sqrt{\{\eta_2'^n\}^2 + \{\alpha\delta_2^n\}^2})^{4/3} \\ (\xi\sqrt{\{\eta_n'^1\}^2 + \{\alpha\delta_n^1\}^2})^{4/3} & (\xi\sqrt{\{\eta_n'^2\}^2 + \{\alpha\delta_n^2\}^2})^{4/3} & 0 \end{pmatrix} \begin{pmatrix} x_1 \\ \dots \\ x_n \end{pmatrix}$$

$$\delta_i^j = \frac{1}{a}\left[\frac{da_i^j}{dx_i^j}\right]$$

$$\eta_2'^1 = \frac{1}{\mu}\left[\frac{d\mu_i^j}{dx_i^j}\right] \Big/ (1 + 0.5\frac{1}{\mu}\left[\frac{d\mu_i^j}{dx_i^j}\right])$$

$$\frac{d\mu_1^2}{dx_1^2} = \left((x_1, x_2 \dots, x_n)\begin{pmatrix}\mu_1 \\ \mu_2 \\ \mu_n\end{pmatrix}(x_1 - \delta x, x_2 + \delta x \dots, x_n)\right)\frac{1}{\delta x}$$

where x_i denotes the atomic concentration of the i-component, μ_i denotes the shear modulus of the i-component, α =12.2, ξ = 2, F_τ=3 is the Taylor factor and Z= 0.0026. The values of the atomic radii, shear modulus and bulk modulus of the elements were used in the calculations are given in Table 2. The values of SSH were specified after production of the model alloys using their measured chemical compositions (Table 1). The result of calculating SSH for the model alloys at 20 °C and 600 °C are given in Table 3.

Meanwhile, XRD analysis showed that only alloys A2, A4 and A7 comprised a single phase structure with a BCC lattice. Other alloys contained intermetallic phases. The actual phase composition is in good agreement with the results of modeling by Thermo-Calc.

Table 2. Values of atomic radii, shear modulus and bulk modulus used in calculations.

Elements	Atom radius at 20/600 °C (pm)	Shear modulus at 20/600 °C (GPa)	Bulk modulus at 20/600 °C (GPa)
Al	143.17/145.55	95/95	86/7/67.7
Cr	124.91/125.49	103.7/93.7	136.4/114.9
Nb	142.9/143.24	37.3/38.8	170.5/165.2
Ti	146.15/148.34	74/43	97/81.52
V	131.6/131.74	48.1/39.1	157.1/139.3
Zr	160.25/160.89	60.2/37.8	91.7/79.2

The correspondence between the calculated values of the yield strength of the model alloys and its actual value is shown in Figure 2. The results of prediction agreed well with the experimental values. For most of the model alloys, the difference between the calculated and experimental values of the yield strength did not exceed 15%.

Table 3. Mechanical properties of model alloys at 20 and 600 °C.

Alloys	Compressive yield strength at 20 °C (MPa)	Microhardness (GPa)	Yield stress calculated from microhardness at 20 °C (MPa)	Predicted SSH at 20 °C (MPa)	Compressive yield strength at 600 °C (MPa)	Predicted SSH at 600 °C (MPa)
A1	1070	5.42	1316	1417	1093	1284
A2	948	5.80	1410	902	1069	769
A3	1608	6.38		1804	1385	1549
A4	1337	5.41	1314	1205	1096	967
A5	1295	5.30		1196	1113	1026
A6	1290	4.79		1353	1048	1107
A7	998	4.86		1221	895	929
A8	1049	5.45	1323	1335	1122	1001

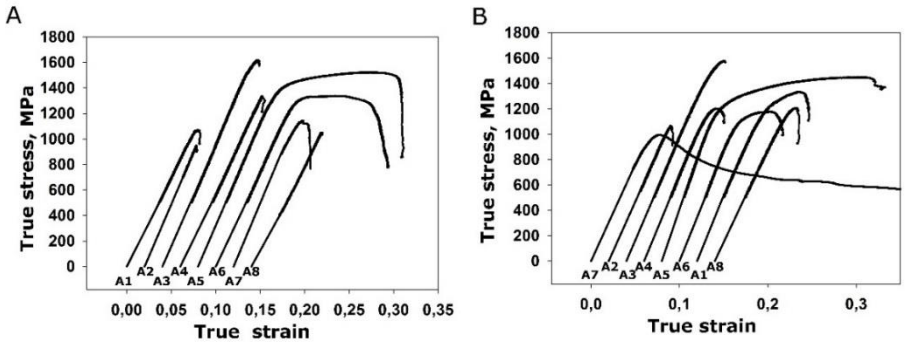

Figure 1. Compressive stress-strain curves for the model alloys at 20 °C (A) and 600 °C(B).

Figure 1 shows the compressive true strain-true stress curves for the model alloys at 20 and 600 °C. The detailed data on the mechanical properties of the model alloys are listed in Table 3. The yield strengths of the model alloys at 20 °C are in a range from 998 MPa for A7 alloy to 1608 MPa for A3 alloy. But most of the model alloys show the yield strengths at room temperature around 1300 MPa. Ductility over 1% was showed only by A5, A6 and A7 alloys (16.6, 13.8 and 3.6% respectively). A1, A2, A4 and A7 alloys fractured in the elastic region. For those specimens, which fractured brittle at room temperature, the yield strengths were recalculated from the microhardness values. The ratio between microhardness and yield strengths was evaluated using the corresponding values for the more ductile alloys (i.e. A5, A6 and A7). This ratio was found to be 0.2428 and the estimated yield strengths values for A1, A2, A4 and A8 are 1316, 1410, 1314 and 1323 MPa, respectively. At 600 °C as well as at 20 °C, the highest and the lowest values of the yield strengths were showed by A7 and A3 alloys

(1385 and 895 MPa, respectively). The yield strengths of the other model alloys were around 1100 MPa. Only A1, A5 and A7 alloys showed ductility over 5% (17.2%, 5.5% and more 50%, respectively), but none of the alloys broke out in the elastic region. The best strength/ductility ratio at both 20 °C and 600 °C was demonstrated by A1 and A6 alloys.

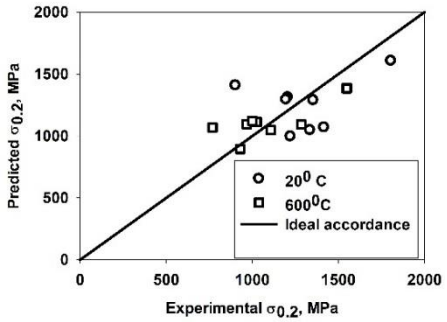

Figure 2. Experimental and predicted yield strengths at 20 and 600 °C.

4. Conclusion

The prediction of the solid solution hardening based on the atom radii and elastic modules misfit showed good agreement with the experimental values of the yield strength at 20 and 600 °C. The combination of approaches for predicting the phase composition of HEA(CALPHAD and thermodynamically rules) with the calculation of solid-solution hardening is promising for quick searching for high entropy alloys with a given phase composition and strength properties. For most of the model alloys, the difference between the predicted and experimental values of the yield strength at both 20 °C and 600 °C was found to be less than 15%.

Acknowledgments

This research was carried out with the financial support of the Russian Science Foundation, Project No. 19-79-30066

References

[1] Yeh J-W, Chen S-K, Lin S-J, Gan J-Y, Chin T-S, Shun T-T, Tsau C-H and Chang S-Y 2004 *Adv. Eng.Mater*. **8** 299-303
[2] Zhang Y, Zhou Y J,Lin J P, Chen G L and Liaw P K 2008 *Adv. Eng.Mater.* **10** 534-8
[3] Zhang Y, Zuo T T, Tang Z, Gao M C, Dahmen K A, Liaw P K and Lu Z P 2014 *Prog.Mater.Sci.***61** 1-93
[4] Wu Y D, Cai Y H, Wang T, Si J J, Zhu J, Wang Y D and Hui X D 2014 *Mater.Lett* **130** 277-80
[5] Stepanov N D, Yurchenko N Y, Skibin D V, Tikhonovsky M A and Salishchev G A 2015 *J. Alloys Compd*. 266-80
[6] Toda-Caraballo I, del-Castillo P E J R-D 2015 *Acta Mater*. **85** 14-23
[7] Toda-Caraballo I 2017 *Scripta Mater*. **127** 113-7
[8] Wang Z, Fang Q, Li J, Liu B and Liu Y 2018 *J.Mater. Sci. Technol.* **32** 349-54
[9] Coury F G, Kaufman M and Clarke A J 2019 *Acta Mater* **175** 66-81
[10] Fleischer R L 1963 *Acta Metall.* **11** 203-9
[11] Labush R 1972 *Acta Metall.***20** 917-27
[12] Guo S 2015 *J. Matter. Sci. Technol.* **31** 1223-30